Nanoshell Arrays

DOI: 10.1002/anie.200702072

Plasmonic Nanoshell Arrays Combine Surface-Enhanced Vibrational Spectroscopies on a Single Substrate**

*Hui Wang, Janardan Kundu, and Naomi J. Halas**

The collective oscillations of free electrons in metallic materials—known as surface plasmons—have properties determined by the structure of the metal, and can ultimately be tailored to impart new optically-induced functionalities into materials for specific practical uses. For subwavelength metallic structures, the geometry of the structure controls the resonance frequencies of its surface plasmons. These structured metallic materials, in turn, provide new and unique methods for manipulating light, giving rise to a whole set of new properties and applications.[1–6]

The enhancement by a nearby metallic structure of molecular spectroscopies, such as Raman scattering, infrared absorption, UV/Vis absorption, and fluorescence, is a particularly interesting and useful phenomenon.[7–14] The optical excitation of plasmon resonances supported by metallic nanostructures gives rise to strongly enhanced electromagnetic fields at their surfaces,[15] which are largely responsible for the observed spectroscopic enhancements. Enhancements of Raman spectroscopy and infrared absorption spectroscopy are of particular interest due to the usefulness of these methods for elucidating molecular structures.[16] Because of their virtually complementary selection rules, it would, in fact, be far preferable to use these two spectroscopies in combination with each other when possible, since together they can provide a complete "chemical fingerprint" for the identification of unknown molecules.

The past decade has witnessed a dramatic resurgence of interest in surface-enhanced spectroscopies,[7] fueled largely by the remarkable discovery that single-molecule sensitivity in surface-enhanced Raman spectroscopy (SERS) indeed appears achievable for molecules dispersed within random aggregates of metallic nanoparticles.[8,17–20] This enormous Raman enhancement has since been identified as arising from molecules positioned in the junctions between directly adjacent nanoparticles, a geometry which gives rise to huge field intensities between the two particles when illuminated, a configuration also known as a "hot spot".[17,18,20–22] In contrast to SERS, surface-enhanced infrared absorption (SEIRA) spectroscopy has not received nearly the same attention.[23–26] This is primarily for two reasons: compared to SERS, more modest enhancements are anticipated, since SEIRA depends quadratically on the local field, not quartically as does SERS; moreover, the excitation of large local fields on metallic substrates across the broad range of mid-infrared frequencies needed for SEIRA has not previously been achieved.

The plasmon hybridization picture, an analogy between interacting plasmons and the wave function hybridization of molecular orbital theory,[27–29] provides a simple conceptual framework for the design of plasmon resonant structures that can be useful as substrates for surface-enhanced spectroscopies. For example, directly adjacent pairs of nanoparticles can be regarded as plasmonic "dimers", where excitation of hybridized "bonding" dimer plasmons gives rise to the strong interparticle field enhancement that results in the large SERS enhancements of the hot-spot geometry.[30] Ordered arrays of metallic nanospheres with sub-10-nm interparticle gaps have been shown to provide SERS enhancements by the same mechanism.[31] Metallic nanoparticles with geometrically tunable plasmon resonances, such as metallic nanoshells,[32] can also serve as optimized substrates for SERS when the Raman excitation laser wavelength is within the linewidth of plasmon resonance of the individual nanoparticles.[33,34] For metallic nanoshells, the field enhancement essentially arises from strongly interacting plasmons on the inner and outer surfaces of the metallic shell layer.[27,35] The integrated SERS enhancement of an individual nanoshell approaches that observed for hot spots of adjacent solid metallic nanoparticle pairs.[36]

Herein we report a specifically designed, subwavelength-structured metallic substrate that simultaneously enhances two complementary vibrational spectroscopies, namely, Raman scattering and infrared absorption spectroscopy, by introducing plasmon resonances in the two diverse frequency regions required for both spectroscopies. Our strategy is based on the assembly of near-infrared-resonant nanoshells into a 2D periodic array with sub-10-nm interparticle gaps. The resulting nanoshell array is a unique structure which has hot spots in the interparticle junctions that enhance SERS at near-infrared wavelengths, and simultaneously provide broadband mid-infrared hot spots for SEIRA at precisely the same locations on the substrates.

[*] H. Wang, J. Kundu, Prof. N. J. Halas
Department of Chemistry, Department of Electrical and Computer Engineering, and the Laboratory for Nanophotonics
Rice University
6100 Main Street, Houston, TX 77005-1892 (USA)
Fax: (+1) 713-348-5686
E-mail: halas@rice.edu
Homepage: http://www.ece.rice.edu/~halas

[**] We thank Peter Nordlander for insightful discussions on this subject. This work is supported by the Air Force Office of Scientific Research Grant F49620-03-C-0068, the National Science Foundation (NSF) grants EEC-0304097 and ECS-0421108, the Texas Institute for Bio-Nano Materials and Structures for Aerospace Vehicles funded by NASA Cooperative Agreement No. NCC-1-02038, the Robert A. Welch Foundation Grants C-1220, and the Multidisciplinary University Research Initiative (MURI) Grant W911NF-04-01-0203.

Supporting information for this article is available on the WWW under http://www.angewandte.org or from the author.

The major steps involved in the fabrication of Au nanoshell arrays are illustrated schematically in Figure 1a. Au nanoshells were fabricated by following a previously reported seed-mediated electroless plating method and then purified by dialysis. The dialyzed nanoshells were functionalized with the surfactant cetyltrimethyl ammonium bromide (CTAB) and subsequently redispersed in water to form colloidal solutions with desired particle concentrations. Applying droplets of nanoshell solution to a substrate and allowing the solvent to evaporate under ambient conditions resulted in the formation of hexagonally packed nanoshell arrays, which maintain an interparticle spacing established by the bilayers of CTAB that surround each nanoshell as the interparticle spacer.

The nanoshells organize into hexagonally close packed (hcp) structures with typical domain sizes ranging from several tens of micrometers to over two hundred micrometers (Figure 1b–d). CTAB plays a critical role both in the self-assembly of these arrays as well as in defining the local electromagnetic properties of the nanoshell array structures. The CTAB molecules form bilayer structures on the surface of Au nanoparticles,[31,37,38] which result in a net positive charge on the nanoparticle surfaces and provide a net repulsive interaction between the nanoparticles to prevent random disordered aggregation during solvent evaporation. Control experiments with unfunctionalized nanoshells only resulted in the formation of disordered aggregates. The CTAB bilayers also define the spacing between neighboring nanoshells and result in an average interparticle spacing determined to be about 8 nm, consistent with the reported thickness of approximately 4.4 nm for a CTAB bilayer. These sub-10-nm gaps are instrumental for inducing the strong plasmon coupling that results in the specific electromagnetic properties of this array geometry.

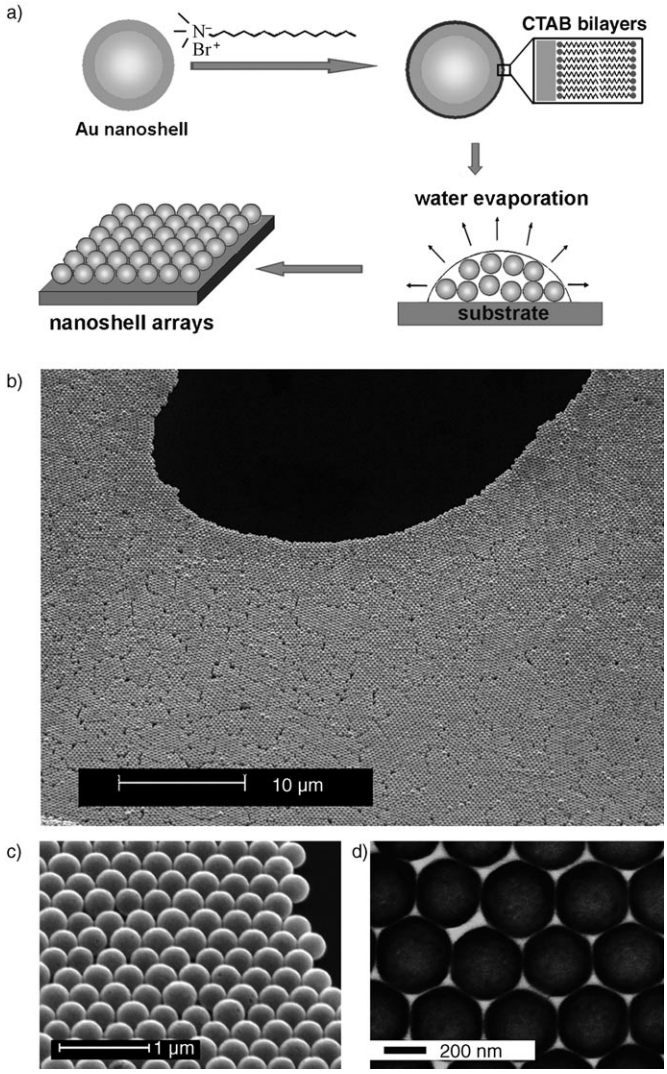

Figure 1. a) Fabrication of Au nanoshell arrays. b, c) SEM images of nanoshell arrays formed by drying 40 μL of aqueous solutions of CTAB-capped Au nanoshells on silicon wafers. The core radius of the nanoshells is 150±12 nm, and the shell thickness is 22±1 nm. d) TEM image of the nanoshell arrays formed on a TEM grid.

Figure 2 compares the optical extinction spectra of nanoshell arrays with the spectra of the isolated and dispersed constituent nanoshells. These measurements were performed on nanoshell monolayer arrays formed on glass slides with unpolarized light at normal incidence. Nanoshell arrays have two distinct plasmon resonances: a narrow visible or near-infrared band at frequencies corresponding closely to those of the isolated nanoshell plasmons, and in addition, a broad feature extending from the near-infrared well into the mid-infrared region of the spectrum. The two plasmon bands observed for the nanoshell arrays arise from the plasmon interactions between neighboring nanoshells in the arrays. How the individual nanoshell plasmons interact with each other to form hybridized nanoshell array plasmons can be understood by applying the plasmon hybridization model to multinanoparticle systems.[39,40] When nanoshells are close-packed into an array structure, the dipolar plasmons of the individual nanoshells strongly intermix to form a hybridized plasmon band, evolved from the dipolar plasmon mode, which disperses strongly to lower energies corresponding to infrared wavelengths. The individual nanoshell quadrupole resonances, on the other hand, also intermix, but only weakly, do not disperse upon hybridization, and give rise to a plasmon band in the near-infrared that appears quite similar in both wavelength and lineshape to the dipole plasmon of the individual nanoshell particles.

In addition to the new features arising in the far-field extinction spectra, the interparticle plasmon coupling in the nanoshell arrays produces intense near-field enhancements at the junctions between neighboring nanoshells, and creates uniform periodic densities of hot spots for surface-enhanced spectroscopies. Theoretical simulations of the near-field properties of nanoshell arrays by using the finite difference time domain (FDTD) method[41,42] indicate that the localized field enhancements ($|E|/|E_0|$) inside interparticle junctions are approximately 30 both in the near infrared and over a broad range (ca. 2–8 μm in wavelength) in the mid-infrared. Such large field enhancements in both near- and mid-infrared are achievable only when the interparticle spacing is within the sub-10-nm range. In comparison, isolated nanoshells provide much weaker field enhancements, with maximum enhancements of approximately fivefold for nanoshell plasmons in the near-infrared and negligible field enhancements

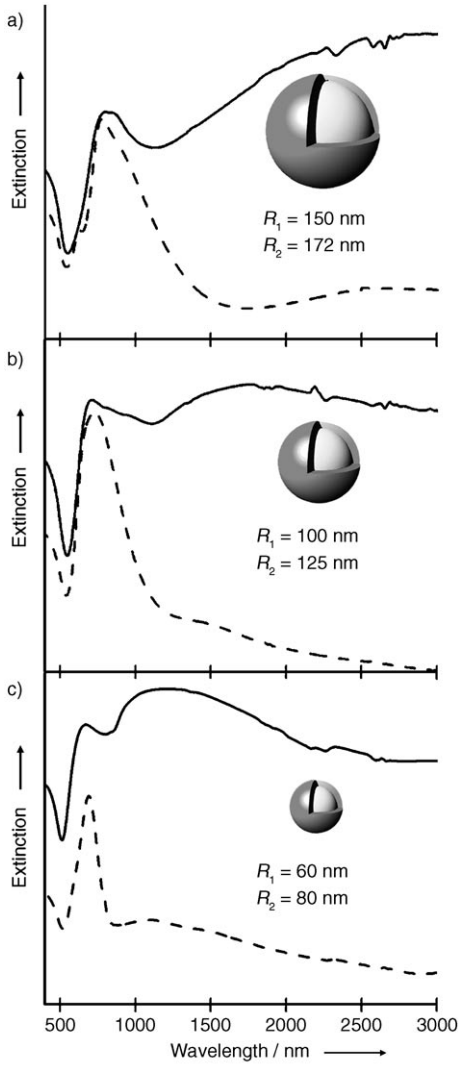

Figure 2. Normal-incidence extinction spectra of monolayer nanoshell arrays (solid curves) and submonolayers of isolated nanoshells (dashed curved) supported on glass slides. a) Au nanoshells with 150-nm core radius and 22-nm shell thickness, b) Au nanoshells with 100-nm core radius and 25-nm shell thickness, and c) Au nanoshells with 60-nm core radius and 20-nm shell thickness.

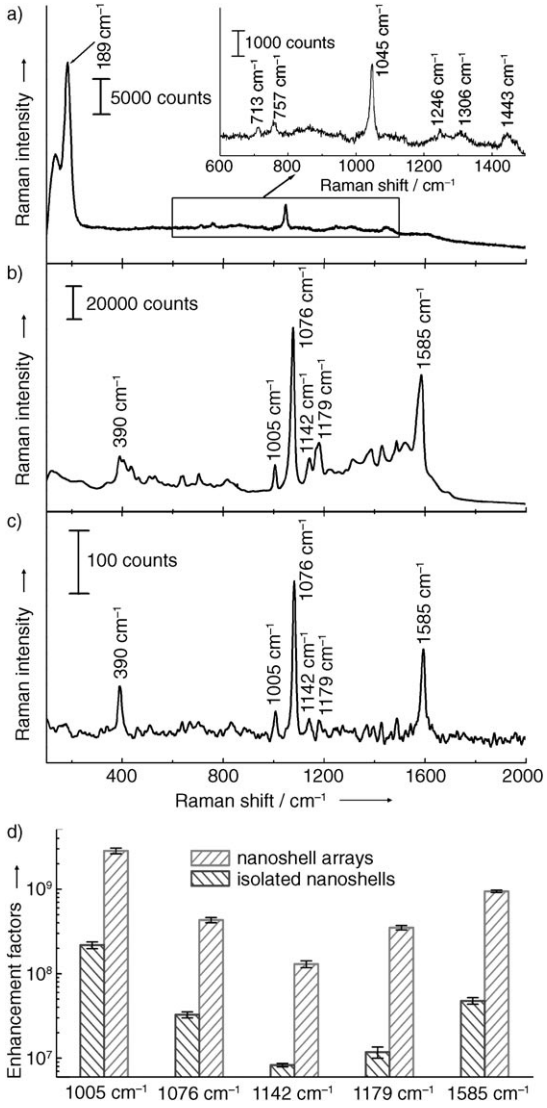

Figure 3. SERS performance of the nanoshell arrays. SERS spectrum of a) CTAB and b) *p*MA on nanoshell (150-nm core radius, 22-nm shell thickness) monolayer arrays. c) SERS spectrum of *p*MA on the isolated nanoshells (150-nm core radius, 22-nm shell thickness). The coverage of the submonolayer of isolated nanoshells was determined to be 212 ± 15 particles in each beam spot according to the SEM images. d) Empirical SERS enhancement factors of *p*MA adsorbed on nanoshell arrays and the isolated nanoshells.

in the mid-infrared. The nanoshell array structure turns out to be uniquely suited as an integrated SERS-SEIRA substrate, by providing hot spots in the interparticle junctions that enhance both SERS at near-infrared wavelengths and SEIRA at mid-infrared wavelengths. It is this property that enables the observation of large, reproducible SERS and SEIRA enhancements on the same substrate.

The nanoshell arrays were evaluated as SERS-SEIRA substrates by using a nonresonant adsorbate molecule, namely, *para*-mercaptoaniline (*p*MA), which is ideal for spectroscopic quantification on these substrates because it displaces CTAB on Au surfaces and is known to form self-assembled monolayers (SAMs) on Au surfaces with a known packing density.[31,43] Figure 3a shows the SERS spectrum of CTAB ($\lambda_{exc} = 785$ nm) on the surface of the as-fabricated nanoshell arrays, with a strong characteristic feature at 189 cm^{-1} corresponding to the Au–Br mode. On complete displacement of the CTAB molecules, the Au–Br mode and all the SERS modes of CTAB disappear, while the SERS modes of *p*MA and the Au–S bond at 390 cm^{-1}, which become evident in the SERS spectrum (Figure 3b), indicate the formation of saturated SAMs of *p*MA on the nanoshell array surfaces (see detailed peak assignments in the Supporting Information). The SERS spectra of *p*MA on the nanoshell arrays are highly reproducible at different sites on a substrate with a standard deviation of less than 10%. For comparison, the SERS spectrum of saturated *p*MA SAMs on the surface of isolated nanoshells is also shown in Figure 3c. Empirical signal enhancement factors were determined by comparing ratios of the intensity of SERS modes to the

corresponding unenhanced signals from neat *p*MA films of known thickness. Both the SERS and normal Raman intensities are normalized by the number of molecules being probed. As presented in Figure 3d, the empirical enhancement factors of *p*MA on the nanoshell arrays are on the order of 10^8–10^9, 10 to 20 times larger than what is achievable on isolated nanoshells. The SERS enhancements obtained on these nanoshell arrays are of the same order of magnitude as those achieved on solid Au nanosphere arrays.[31] These measurements represent the overall array response, not the localized enhancements inside the interparticle junctions. Finite-difference time-domain (FDTD) calculations for arrays of smooth nanoshells show that the maximum local $(|E|/|E_0|)^4$ enhancement factor in the high-field junctions of these arrays is on the order of 10^6, which enables these substrates to approach zeptomolar molecular detection limits. This is a conservative number, sensitive to further enhancements by closer internanoparticle spacings and localized asperities on the surface of individual nanostructures.

The broad plasmon of the nanoshell array in the mid-infrared region enhances SEIRA quite well. Figure 4a shows a normal IR spectrum of neat *p*MA film (0.60 mm thick) supported on a silicon wafer and a typical SEIRA spectrum of SAMs of *p*MA formed on the nanoshell array surfaces (see detailed peak assignments in Supporting Information). Utilizing the nanoshell arrays as SEIRA substrates enables the acquisition of high-quality SEIRA spectra of *p*MA across much of the IR fingerprinting region, and enhances several characteristic vibrational modes that correspond to most of the normal IR features of the molecule. The most striking difference between SEIRA and normal IR spectra is the highly asymmetric, characteristic Fano-type lineshape of SEIRA, which is believed to be due to the interaction between the molecular vibrations and the electronic excitations in the metallic substrates.[44–48] The SEIRA enhancement factors were determined by directly comparing the ratios of the normalized intensity of SEIRA modes to the corresponding unenhanced IR signals from neat *p*MA films, in precisely the same manner that we determined the SERS enhancements on the same substrate. The SEIRA enhancement factors of each of the observed IR modes of *p*MA are shown in Figure 4b. For this substrate and measurement approach, the SEIRA enhancement factors of *p*MA on the nanoshell arrays for all observed modes are on the order of 10^4. We have also performed SEIRA measurements on *p*MA SAMs on a planar Au surface and isolated nanoshells. However, no signals were observed, as neither the planar Au surface nor isolated nanoshells can provide the large local field enhancements associated with the broadband mid-infrared plasmons. The remarkably large enhancement factors and high reproducibility of the SEIRA spectra obtained on these substrates open new opportunities for the broader development of SEIRA as a reliable and reproducible spectroscopic method.

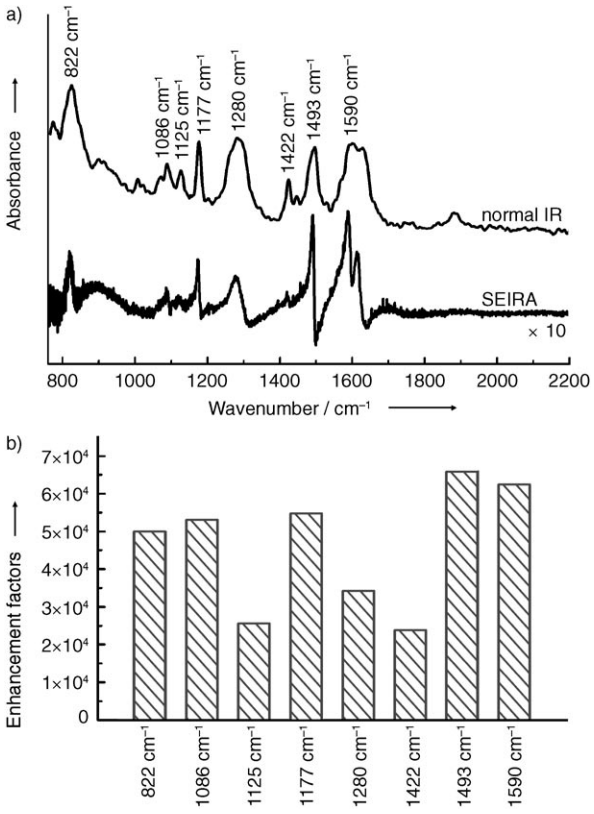

Figure 4. SEIRA performance of the nanoshell arrays. a) Normal IR spectrum of pure *p*MA and SEIRA spectrum of *p*MA SAMs on the nanoshell arrays. b) SEIRA enhancement factors of different IR modes calculated on the basis of the experimental spectra.

The nanoshell array substrates reported herein provide a new, multifunctional platform for chemical sensing applications by enhancing both RS and IRA spectroscopy. Integrating SERS and SEIRA on a single substrate will enable the identification of unknown molecules by combining both surface-enhanced vibrational spectroscopies, allowing more detailed investigations of molecular structure, orientation, and conformation, as well as adsorbate–substrate and adsorbate–adsorbate interactions. This substrate geometry also provides a system for detailed and highly reproducible correlations between surface-field properties and spectroscopic enhancements, which should enhance our ability to unravel the complex mechanisms involved in surface-enhanced spectroscopic processes.

Experimental Section

The Au nanoshells used in the present work were fabricated by following a previously reported wet-chemistry method.[49] The as-fabricated nanoshells were further purified by dialysis. In a typical procedure, 40 mL of aqueous nanoshell solution was transferred into a regenerated-cellulose membrane dialysis bag (Spectra-Por, molecular weight cutoff (MWCO) 6000–8000). The bag was then suspended in a reservoir of Milli-Q water (Millipore, Billerica, MA) and gently stirred overnight. The dialyzed nanoshells were collected by centrifugation and redispersed in 25 mM aqueous CTAB (Sigma-Aldrich) solution for 1 h. The CTAB-capped nanoshells were then collected by centrifugation and redispersed in Milli-Q water to form colloidal solutions with desired particle concentrations. The assembly of the nanoshells into close-packed arrays was accomplished by depositing a droplet of colloidal solution (40 μL) onto a substrate surface (silicon wafer, glass slide, ITO glass, or TEM grid) and allowing it to dry undisturbed under ambient conditions. The pattern morphologies of the nanoshell arrays were dependent on the particle concentration of the nanoshell solutions. At very low particle concentrations, only

isolated small monolayer domains of arrays with short-range order could be formed on the substrates. Increasing the particle concentration resulted in an increase in the domain size as the initially separated domains began to coalesce with each other to form continuous long-range-ordered monolayers. The optimum concentration for the fabrication of long-range-ordered monolayer arrays is 2.40×10^9 particles per milliliter for the nanoshells with inner and outer radii of $R_1 = 150$ nm and $R_2 = 172$ nm, respectively. Further increase in the particle concentration resulted in the formation of double-layer, triple-layer, and eventually multilayer arrays. The submonolayers of isolated nanoshells were prepared by immobilizing the nanoshells onto poly(4-vinylpyridine)-functionalized glass by following a previously reported protocol.[33]

Optical extinction spectra were obtained with a Cary 5000 UV/Vis/NIR spectrophotometer. SEM measurements were performed on a Phillips FEI XL-30 environmental scanning electron microscope. TEM images were obtained with a JEOL JEM-2010 transmission electron microscope. The samples for SERS and SEIRA measurements were prepared by evaporating 10 μL of a 20 μM solution of *p*MA in ethanol on the surface of the nanoshell arrays or isolated nanoshells. Raman spectra were obtained with a Renishaw micro-Raman spectrometer using a 785 nm excitation laser (250 mW), line-focus mode (beam size 4×60 μm), 50× objective, 0.05% laser power, and 10-s acquisition time. The laser power focused on the samples was measured to be 0.035 mW when the 50× objective and 0.05% laser power were used. SEIRA measurements were performed with an FTIR microscope (Nexus 670, Thermo Nicolet) equipped with a liquid-nitrogen-cooled MCT (HgCdTe) detector. The SEIRA spectra were obtained from the coaddition of 256 scans with 4-cm^{-1} resolution in reflection mode.

Received: May 10, 2007
Revised: July 20, 2007
Published online: October 23, 2007

Keywords: IR spectroscopy · nanostructures · Raman spectroscopy · self-assembly · surface-enhanced spectroscopy

[1] W. L. Barnes, A. Dereux, T. W. Ebbesen, *Nature* **2003**, *424*, 824.
[2] S. A. Maier, M. L. Brongersma, P. G. Kik, S. Meltzer, A. A. G. Requicha, H. A. Atwater, *Adv. Mater.* **2001**, *13*, 1501.
[3] S. A. Maier, H. A. Atwater, *J. Appl. Phys.* **2005**, *98*, 011101.
[4] E. Ozbay, *Science* **2006**, *311*, 189.
[5] J. B. Pendry, *Phys. Rev. Lett.* **2000**, *85*, 3966.
[6] T. W. Ebbesen, H. J. Lezec, H. F. Ghaemi, T. Thio, P. A. Wolff, *Nature* **1998**, *391*, 667.
[7] M. Moskovits, *Rev. Mod. Phys.* **1985**, *57*, 783.
[8] S. Nie, S. R. Emory, *Science* **1997**, *275*, 1102.
[9] Y. W. C. Cao, R. C. Jin, C. A. Mirkin, *Science* **2002**, *297*, 1536.
[10] R. Elghanian, J. J. Storhoff, R. C. Mucic, R. L. Letsinger, C. A. Mirkin, *Science* **1997**, *277*, 1078.
[11] M. Osawa, *Bull. Chem. Soc. Jpn.* **1997**, *70*, 2861.
[12] K. Aslan, I. Gryczynski, J. Malicka, E. Matveeva, J. R. Lakowicz, C. D. Geddes, *Curr. Opin. Biotechnol.* **2005**, *16*, 55.
[13] G. Schneider, G. Decher, N. Nerambourg, R. Praho, M. H. V. Werts, M. Blanchard-Desce, *Nano Lett.* **2006**, *6*, 530.
[14] F. Tam, G. P. Goodrich, B. R. Johnson, N. J. Halas, *Nano Lett.* **2007**, *7*, 496.
[15] U. Kreibig, M. Vollmer, *Optical Properties of Metal Clusters*, Springer, Berlin, **1995**.
[16] B. Schrader, *Infrared and Raman Spectroscopy: Methods and Applications*, Weinheim, New York, **1995**.
[17] K. Kneipp, Y. Wang, H. Kneipp, L. T. Perelman, I. Itzkan, R. R. Dasari, M. S. Feld, *Phys. Rev. Lett.* **1997**, *78*, 1667.
[18] A. M. Michaels, M. Nirmal, L. E. Brus, *J. Am. Chem. Soc.* **1999**, *121*, 9932.
[19] A. M. Michaels, J. Jiang, L. Brus, *J. Phys. Chem. B* **2000**, *104*, 11965.
[20] H. X. Xu, E. J. Bjerneld, M. Kall, L. Borjesson, *Phys. Rev. Lett.* **1999**, *83*, 4357.
[21] D. A. Genov, A. K. Sarychev, V. M. Shalaev, A. Wei, *Nano Lett.* **2004**, *4*, 153.
[22] S. J. Lee, A. R. Morrill, M. Moskovits, *J. Am. Chem. Soc.* **2006**, *128*, 2200.
[23] M. Osawa, *Top. Appl. Phys.* **2001**, *81*, 163.
[24] A. Hartstein, J. R. Kirtley, J. C. Tsang, *Phys. Rev. Lett.* **1980**, *45*, 201.
[25] T. R. Jensen, R. P. Van Duyne, S. A. Johnson, V. A. Maroni, *Appl. Spectrosc.* **2000**, *54*, 371.
[26] K. R. Rodriguez, S. Shah, S. M. Williams, S. Teeters-Kennedy, J. V. Coe, *J. Chem. Phys.* **2004**, *121*, 8671.
[27] E. Prodan, C. Radloff, N. J. Halas, P. Nordlander, *Science* **2003**, *302*, 419.
[28] H. Wang, D. W. Brandl, P. Nordlander, N. J. Halas, *Acc. Chem. Res.* **2007**, *40*, 53.
[29] E. Prodan, A. Lee, P. Nordlander, *Chem. Phys. Lett.* **2002**, *360*, 325.
[30] P. Nordlander, C. Oubre, E. Prodan, K. Li, M. I. Stockman, *Nano Lett.* **2004**, *4*, 899.
[31] H. Wang, C. S. Levin, N. J. Halas, *J. Am. Chem. Soc.* **2005**, *127*, 14992.
[32] E. Prodan, P. Nordlander, *Nano Lett.* **2003**, *3*, 543.
[33] J. B. Jackson, N. J. Halas, *Proc. Natl. Acad. Sci. USA* **2004**, *101*, 17930.
[34] A. J. Haes, C. L. Haynes, A. D. McFarland, G. C. Schatz, R. R. Van Duyne, S. L. Zou, *MRS Bull.* **2005**, *30*, 368.
[35] E. Prodan, P. Nordlander, *J. Chem. Phys.* **2004**, *120*, 5444.
[36] C. E. Talley, J. B. Jackson, C. Oubre, N. K. Grady, C. W. Hollars, S. M. Lane, T. R. Huser, P. Nordlander, N. J. Halas, *Nano Lett.* **2005**, *5*, 1569.
[37] B. Nikoobakht, Z. L. Wang, M. A. El-Sayed, *J. Phys. Chem. B* **2000**, *104*, 8635.
[38] C. J. Orendorff, P. L. Hankins, C. J. Murphy, *Langmuir* **2005**, *21*, 2022.
[39] D. W. Brandl, C. Oubre, P. Nordlander, *J. Chem. Phys.* **2005**, *123*, 024701.
[40] D. W. Brandl, N. A. Mirin, P. Nordlander, *J. Phys. Chem. B* **2006**, *110*, 12302.
[41] C. Oubre, P. Nordlander, *J. Phys. Chem. B* **2004**, *108*, 17740.
[42] P. Nordlander, personal communication.
[43] N. Mohri, S. Matsushita, M. Inoue, K. Yoshikawa, *Langmuir* **1998**, *14*, 2343.
[44] A. Priebe, M. Sinther, G. Fahsold, A. Pucci, *J. Chem. Phys.* **2003**, *119*, 4887.
[45] O. Krauth, G. Fahsold, A. Pucci, *J. Chem. Phys.* **1999**, *110*, 3113.
[46] O. Krauth, G. Fahsold, N. Magg, A. Pucci, *J. Chem. Phys.* **2000**, *113*, 6330.
[47] D. A. Heaps, P. R. Griffiths, *Vib. Spectrosc.* **2006**, *42*, 45.
[48] N. Goutev, M. Futamata, *Appl. Spectrosc.* **2003**, *57*, 506.
[49] S. J. Oldenburg, R. D. Averitt, S. L. Westcott, N. J. Halas, *Chem. Phys. Lett.* **1998**, *288*, 243.

